

Heavy Quark and Sparticle Phenomenology

V. Barger

Physics Department, University of Wisconsin

Madison, Wisconsin 53706, USA

1. Introduction

Data from the CERN $p\bar{p}$ collider provide a new avenue for the study of heavy-quark production and possibly also provide the first indication for the sparticles of supersymmetry. This discussion of the associated phenomenology begins with charm and bottom quarks, proceeds to the strategies that lead to top quark identification, and concludes with possible supersymmetry scenarios to explain the events observed by the UA1 collaboration with large missing transverse momentum. A common thread is the $2 \rightarrow 2$ and $2 \rightarrow 3$ parton mechanisms for production of heavy particles. We find that calculations of charm and bottom production by the $O(\alpha_s^2)$ and $O(\alpha_s^3)$ fusion subprocesses provides a reasonable first description of single muon and non-isolated dimuon events, but do not account for enhanced charm in jets. The top quark search relies on the selective suppression by lepton isolation requirements of b and c quark backgrounds, calculated from fusion. The calculated cross sections for sparticle production are similarly based on the validity of the $2 \rightarrow 2$ fusion mechanism.

2. Charm and Bottom Production

Heavy-quark production at large p_T or in the central region is nominally assumed to be dominated by the fusion subprocesses

$$\begin{array}{cc}
 O(\alpha_s^2) & \left\{ \begin{array}{l} q\bar{q} \rightarrow Q\bar{Q} \\ gg \rightarrow Q\bar{Q} \end{array} \right. \\
 (2 \rightarrow 2) & \\
 O(\alpha_s^3) & \left\{ \begin{array}{l} q\bar{q} \rightarrow gQ\bar{Q} \\ qg \rightarrow qQ\bar{Q} \\ gg \rightarrow gQ\bar{Q} \end{array} \right. \\
 (2 \rightarrow 3) &
 \end{array}$$

where $Q = c, b$ or t . Inasmuch as fusion contributions are inadequate¹ to explain the large diffractive charm cross section at low p_T observed at ISR energies, it is important that these mechanisms be tested at high p_T with

data from the CERN $p\bar{p}$ collider. Our present ability to predict more esoteric phenomena, such as the cross sections for the production of supersymmetric particles, depends on the dominance of these lowest-order QCD subprocesses.

These perturbative QCD calculations have several inherent ambiguities. There are various reasonable choices for the argument of the running coupling $\alpha_s(Q^2) = 12\pi/[(33 - 2f)\ln(Q^2/\Lambda^2)]$, such as $Q^2 = \hat{s}$ or $Q^2 = p_T^2$, as well as uncertainties in the value of Λ , the number of effective flavors f , and the choice of structure function parametrization. There are cross section enhancements (K factors) from contributions of higher-order diagrams. There are uncertainties associated with the choice of cutoff to regularize the soft and collinear singularities in the $2 \rightarrow 3$ subprocesses; typically a cutoff $p_T(Q\bar{Q}) > 5$ GeV is imposed.^{2,3} The effects of experimental acceptance cuts depend on the fragmentation of the heavy quark to heavy flavored mesons, $Q \rightarrow M(Q\bar{q})$, or baryons. In addition, predictions for lepton final states involve the weak decay matrix and branching fractions for the $M(Q\bar{q}) \rightarrow \ell$ transitions. Taking these various uncertainties into account, the overall uncertainties on the calculated cross sections are at least a factor of two, which must be borne in mind when comparisons are made with data.

The necessary input for heavy quark fragmentation is taken from analyses of heavy quark production in e^+e^- collisions. There the primary fragmentation is well described by the model of Peterson et al.⁴ which gives the fragmentation function $D(z) \propto z(1-z)^2/[(1-z)^2 + \epsilon z]^2$ where $z = p_M/p_Q$ is the momentum fraction evaluated in the subprocess c.m. frame. The parameter ϵ scales with $(m_M)^{-2}$; fits to the e^+e^- data on c and b production are consistent with $\epsilon \approx 0.5 \text{ GeV}^2/m_M^2$. Scaling violation effects in $D(z, Q^2)$ can be ignored at the present level of accuracy. The primary fragmentation of $b \rightarrow B$ is hard, whereas that for $c \rightarrow D$ has a relatively flat z -dependence.

The secondary fragmentation of the charm quark produced in B-meson decays $B \rightarrow c \rightarrow D$, is another matter. The CESR data⁵ on inclusive D production from B decays indicate that this $c \rightarrow D$ fragmentation is hard. To reproduce this observation the secondary fragmentation is described by $D(z) = \delta(1-z)$ in the B meson rest frame.

The charged lepton spectra from B and D decays are well described by the spectator model with V-A bare quark matrix elements. The V-A structure gives a harder $b \rightarrow \ell$ spectrum than $c \rightarrow \ell$. The B decays also have an additional

source of leptons via the cascade $b \rightarrow c \rightarrow \ell$. As a consequence of the harder $b \rightarrow \ell$ spectrum and the harder b fragmentation, leptons from b dominate over those from c .

In the following, typical fusion predictions are compared with recent UAI data.

A. Single muons

Figure 1 shows the predicted components of inclusive single muon production at high p_T from the fusion and electroweak sources. The contributions of the $2 \rightarrow 2$ and $2 \rightarrow 3$ subprocesses are comparable. The summed contributions are in reasonable accord with the UAI measurements.⁶ These data may still contain $\pi, K \rightarrow \mu$ contamination,⁷ so firm conclusions cannot be drawn yet regarding the precision of the agreement.

B. Dimuons

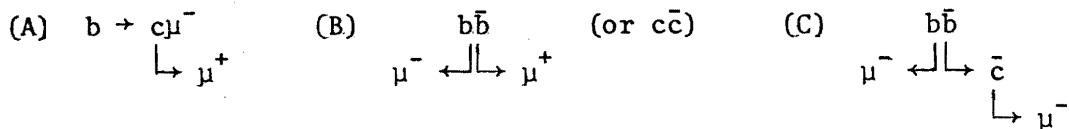
The observation by the UAI collaboration⁸ of dimuon events with invariant dimuon masses in the range 2-22 GeV offers a good opportunity to test fusion expectations for heavy-quark production.^{9,10} Moreover, the Drell-Yan mechanism for electroweak pairs can be tested at higher energy.

The UAI acceptance criteria for dimuon events are $p_T(\mu_i) > 3$ GeV, $p_T(\mu_1) + p_T(\mu_2) > 10$ GeV, and $\eta(\mu_i) < 1.3, 2.0$, respectively. The imposition of these cuts is critical; our calculations⁹ indicate a dimuon acceptance only of order 10^{-3} of the true rate.

It is convenient to consider three categories of heavy-quark sources:

$$(A) \quad m(\mu^+\mu^-) < 4 \text{ GeV} ; \quad (B) \quad m(\mu^+\mu^-) > 4 \text{ GeV} ; \quad (C) \quad \mu^-\mu^- \text{ and } \mu^+\mu^+ .$$

The dimuons in category A are from the same b parent. In B the dimuons come from different primary $b\bar{b}$ or $c\bar{c}$ quarks. In C like-sign dimuons arise from one primary b and one secondary c decay, in the limit of no $B^0-\bar{B}^0$ mixing.



The dimuon cross sections expected⁹ from the various sources are tabulated below for $p\bar{p}$ collisions at $\sqrt{s} = 630$ GeV, assuming no $B^0-\bar{B}^0$ mixing.

	<u>A</u>	<u>B</u>	<u>C</u>
$b\bar{b}$	21 pb	290 pb	100 pb
$b\bar{b}x$	20	145	48
$c\bar{c}$		56	
$c\bar{c}x$		33	
$t\bar{t}$	1	8	4
$W \rightarrow t\bar{b}$	3	14	13
$Z \rightarrow t\bar{t}$	0.1	1.5	1
$Z \rightarrow b\bar{b}$	1.3	3.1	2.5
$Z \rightarrow c\bar{c}$		1	
$DY^{(0)}$		83	
$DY^{(1)}$		112	

Here $b\bar{b}x$, $c\bar{c}x$ denote the $2 \rightarrow 3$ processes; $DY^{(n)}$ denotes the Drell-Yan contributions for zeroth ($n = 0$) and first-order ($n = 1$) QCD, with cuts $m(\mu\mu) > 1$, $p_T(\mu\mu) > 4$ GeV applied to the first-order calculation.

Muons from semileptonic decays of b and c quarks will mostly lie in or near jets, whereas in $\mu^+\mu^-$ events of Drell-Yan origin the muons will generally be isolated; thus muon isolation provides a plausible means for separating heavy-quark and Drell-Yan sources. The b -quark contributions are the dominant heavy-quark source of non-isolated muons. The cross sections at $\sqrt{s} = 630$ GeV are not much higher than those at $\sqrt{s} = 540$ GeV, so the preceding table can be used to estimate the rate from the CERN collider runs at these energies, with a combined integrated luminosity $\int \mathcal{L} dt \sim 0.38 \text{ pb}^{-1}$. Including a dimuon detection efficiency⁸ of $\epsilon \sim 0.26$, the expected number of dimuon events is $N \approx 0.1\sigma(\text{pb})$. The predicted event rates, compared with numbers of UA1 candidate events, are as follows

	<u>Predicted Events</u>	<u>UA1 Dimuon Events</u>
DY	~ 19	13 isolated events (excluding 12 events in J/ψ and T regions)
$Q\bar{Q}$	~ 66	34 non-isolated events

The Drell-Yan results are in reasonable accord with the observed number of isolated $\mu^+\mu^-$ events; the predicted number of heavy flavor events is about a factor of two high, but this discrepancy can be reduced by making specific parameter adjustments (Λ , f , and ϵ).

The calculated ratio of like-sign to unlike-sign dimuons for zero $B^0-\bar{B}^0$ mixing is

$$\sigma(\mu^\pm\mu^\pm)/\sigma(\mu^+\mu^-) = 0.26$$

to be compared with the preliminary experimental ratio 0.3 ± 0.1 for heavy flavor candidate events. Thus at present there is no need for $B^0-\bar{B}^0$ mixing to understand like-sign non-isolated dimuons.

More detailed tests can be made from scatter plots of $p_T(\mu\mu)$ versus $m(\mu\mu)$. Predictions from the b and c quark sources are given in Fig. 2. The acceptance cuts exclude the region $p_T(\mu\mu)^2 + m(\mu\mu)^2 > (10 \text{ GeV})^2$. The highest event concentrations occur for $m \sim 12 \text{ GeV}$ (different parents) or $m \sim 2 \text{ GeV}$ ($\mu^+\mu^-$ from same parents). The spread between these regions is due to the $2 \rightarrow 3$ contributions. The distribution of non-isolated dimuons observed by the UA1 collaboration⁸ seems to be consistent with these expected patterns.

The predicted numbers of heavy-flavor events with both muons isolated is small ($4 \mu^+\mu^-$ and $\sim 0.5 \mu^\pm\mu^\pm$). The 7 observed isolated like-sign dimuon events cannot be explained by heavy flavors without postulating a large number of unlike-sign isolated dimuons of this origin which would destroy all agreement with the Drell-Yan predictions. This anomaly deserves further attention.

C. Charm in jets

The perturbative charm content of QCD jets can be evaluated from the $2 \rightarrow 2$ and $2 \rightarrow 3$ subprocesses for c and b production, with $b \rightarrow c$ decay. QCD predictions¹¹ for inclusive jet cross sections at $\sqrt{s} = 540 \text{ GeV}$ with $|\eta| \leq 1$ are shown in Fig. 3. The dominant source is the $2 \rightarrow 3$ charm subprocess, due to the hard $g \rightarrow c\bar{c}$ transition. The predicted^{11,12} inclusive charm fraction is of order 5% for transverse momenta in the range $10 < p_T < 50 \text{ GeV}$. This is well below early UA1 indications¹³ for a large D^* signal at low z and $p_T = 16\text{-}20 \text{ GeV}$, shown by the data points in Fig. 4, but the data values may come down.¹³ Even if this signal should hold up, the perturbative result may be correct at large z .

D. Summary

The fusion predictions of single muon and dimuon rates are in the ballpark of UA1 observations. The discovery of isolated like-sign dimuons is at present an anomaly. The $p\bar{p}$ collider is a good place to do B physics, and answer the question of whether $B^0-\bar{B}^0$ mixing occurs. Also, it should soon be possible to identify a few dimuon events of $W \rightarrow t\bar{b}$ and $t\bar{t}$ origins. Finally, enhanced charm in jets, if established, would have to be ascribed to non-perturbative QCD effects.

3. Top Quark Identification

Particle physics has entered a new era in which hadron colliders can be used in the search for new particles. Following the W^\pm and Z boson discoveries¹⁴ at the CERN $p\bar{p}$ collider, evidence for the top quark⁶ has been found. The strategies which permit the top quark signal to be identified from the b and c backgrounds are discussed in this section.

The fact that the t quark exists comes as no surprise. It is needed for renormalization in $SU(2) \times U(1)$. Also, without top, the assignment of one linear combination of $-1/3$ charge quarks would be assigned as a weak isosinglet, upsetting the GIM cancellation mechanism and giving a $Zb\bar{s}$ coupling through which neutral current b-quark (and B-meson) decays would occur. The corresponding predicted lower limit¹⁵ $\Gamma(b \rightarrow se^+e^-)/\Gamma(b \rightarrow c\bar{e}\nu) \geq 0.12$ is violated by CESR data¹⁶ (for which the ratio is < 0.046 with 99.9% confidence) indicating that top exists. For a mass less than 60 GeV, top production at appreciable rates is expected¹⁷⁻¹⁹ at the CERN $p\bar{p}$ collider from $W \rightarrow t\bar{b}$ decays and $t\bar{t}$ hadroproduction.

A. Top from W decay

The decay $W \rightarrow t\bar{b}$ followed by the semileptonic decay $t \rightarrow evb$ provides an electron and jets tag for the t quark¹⁷.

$$W \rightarrow t\bar{b} \rightarrow evb\bar{b} \rightarrow e + \cancel{p}_T + n\text{-jets} .$$

With a jet algorithm analogous to that of the UA1 collaboration, in which partons with $\Delta R = [(\Delta\eta)^2 + (\Delta\phi)^2]^{1/2} < 1$ are coalesced and jet recognition thresholds of $p_T(j_1) > 8$ GeV and $p_T(j_2) > 7$ GeV are required, this signal occurs mainly in the one- and two-jet channels. For electron acceptance $p_T(e) > 15$ GeV and electron isolation $\sum p_T(\text{hadrons}) < 1$ GeV in a cone

$\Delta R < 0.4$, the predicted $e + 2$ -jet cross section is $\sigma(ej_1j_2) \approx 20$ (25) pb at $\sqrt{s} = 540$ (630) GeV. For the integrated luminosity of 120 nb^{-1} at $\sqrt{s} = 540$ GeV and 270 nb^{-1} at $\sqrt{s} = 630$ GeV, and a charged lepton detection efficiency of order 0.5, the expected number of electron + 2-jet events from $W \rightarrow t\bar{b}$ is $N(ej_1j_2) \approx 5$ events. The numbers of t candidates reported by the UA1 collaboration at this meeting²⁰ are $N(ej_1j_2) = 9$ events and $N(\mu j_1j_2) = 3$ events.

B. Backgrounds to top from b and c

The $t \rightarrow be\nu$ decay involves large energy release which leads to a wide dispersal of the decay products; consequently there is a good chance of electron isolation. In contrast, a high- p_T electron from $b \rightarrow ce\nu$ decay must have a fast b parent and lie within about 30° of the hadrons into which the c fragments.^{17,19} The only chance of electron isolation in $qq, gg \rightarrow b\bar{b}$ initiated events occurs when b decays into a high- p_T electron and slow hadrons and \bar{b} decays to a narrow hadronic jet. This background is eliminated by requiring electron isolation and two jets.

The $2 \rightarrow 3$ bottom and charm subprocesses such as $gg \rightarrow gb\bar{b}$ are a potentially more dangerous background to the top signal. In a small fraction of such events $b \rightarrow e + \text{slow hadrons}$ escaping the isolation veto, while \bar{b} and g give narrow jets. However, our calculations² indicate that for electron + 2-jet events this background is small compared to $W \rightarrow t\bar{b}$. Moreover, the $2 \rightarrow 3$ subprocesses give mass distributions that are distinctly different from the $W \rightarrow t\bar{b}$ signal. We conclude that the t signal is separable from the b, c backgrounds.

C. Characteristics of $W \rightarrow t\bar{b}$ events

The Jacobian peak of the fast \bar{b} jet is a distinguishing characteristic¹⁷ of the two-body $W \rightarrow t\bar{b}$ decay. The peak of the $p_T(\bar{b})$ distribution occurs at

$$p_{T(\bar{b})\text{ peak}} \approx \frac{1}{2}M_W - \frac{1}{2}\frac{m_t^2}{M_W} .$$

The fast jet (j_1) is almost always the \bar{b} (92% of the time for $m_t = 40$ GeV).²¹ For comparisons with transverse mass distributions it is convenient to replace $p_T(\bar{b})$ with a variable $M_T(\bar{b})$ defined by²¹

$$M_T^2(\bar{b}) \approx M_W^2 - 2M_W p_T(\bar{b})$$

for which the $M_T \geq m_t$ and the Jacobian peak is at

$$M_T(\bar{b}) = m_t .$$

Transverse mass variables^{17,21} are important to the analysis of $W \rightarrow t\bar{b}$ candidate events. The transverse mass of a cluster of particles c and a missing transverse momentum \not{p}_T is defined as

$$[M_T(c\not{p}_T)]^2 \equiv (c_T^0 + \not{p}_T)^2 - (\vec{c}_T + \vec{\not{p}}_T)^2$$

where $c_T^0 = (|\vec{c}_T|^2 + m_c^2)^{1/2}$ and $\not{p}_T = |\vec{\not{p}}_T|$. For the $e\nu$ from $t \rightarrow b e \nu$ decay the kinematic upper bound on the $e\nu$ transverse mass is

$$M_T(e\not{p}_T) \leq m_t - m_b .$$

For the t cluster, the transverse mass for the effective two-body decay $t \rightarrow (be)\nu$ has a sharp Jacobian peak at the upper endpoint

$$M_T(be, \not{p}_T) \leq m_t .$$

Finally, the W cluster has a transverse mass with bound

$$M_T(be\bar{b}, \not{p}_T) \leq M_W .$$

Figure 5 shows predicted idealized transverse distributions, without resolution or jet identification uncertainties. A good diagnostic for events of $W \rightarrow t\bar{b}$ origin is that the peak regions of all M_T and invariant mass distributions should be simultaneously populated. This expectation seems to be borne out by the three-electron and three-muon events of the UA1 83 run,⁶ for $m_t \approx 40$ GeV, as shown in Fig. 6.

D. Top hadroproduction

Another expected top source is $q\bar{q}, gg \rightarrow t\bar{t}$ which also gives electron events with two jets. The calculated $e + 2$ jets cross section from $t\bar{t}$ (with $m_t = 40$ GeV and $K = 1$) is a factor of two or more below the $W \rightarrow t\bar{b}$ contribution; our experience with dimuon rate calculations suggests that this may be an overestimate of the $t\bar{t}$ cross section. The distributions of $t\bar{t}$ origin are

broader with no distinctive peaks near m_t or m_W , as shown in Fig. 6. Nevertheless, on the basis of rate considerations, and the UAl observation of an electron + 3-jet event, it is likely that some of the present t-candidate events are associated with $t\bar{t}$ production.

E. Future

In the near future we can expect the identification of top in dilepton events (e.g. one muon isolated and one muon in a jet). A more precise determination of the top mass is needed. If a $Z \rightarrow t\bar{t}$ event were found, this would establish that $m_t < \frac{1}{2}M_Z \approx 47$ GeV. Microvertex detectors in $p\bar{p}$ experiments will clean up top signals by aiding in b,c identification. A future task is to determine whether diffractive $t\bar{t}$ production occurs in addition to fusion. It is also important to continue to search for other possible new particles that might have masses comparable to top, such as the $Q = -1/3$ member²² of a fourth generation doublet (a,v) or supersymmetry particles.

4. Sparticle Production

Monojets and multijets with large missing transverse momentum (denoted by \not{p}_T) found by the UAl collaboration²³ may be unexplained by standard model backgrounds, especially the events with $\not{p}_T > 40$ GeV. It is possible that these \not{p}_T events are the first signal of the sparticles of supersymmetry. The sparticles invoked to explain the \not{p}_T events are the photino ($\tilde{\gamma}$), gluino (\tilde{g}), and squark (\tilde{q}). The photino is assumed to be light (< 10 GeV); it interacts feebly, escaping undetected at the collider. The missing p_T results from photinos emitted in the decays $\tilde{q} \rightarrow q\tilde{\gamma}$ or $\tilde{g} \rightarrow q\bar{q}\tilde{\gamma}$. Current calculations of sparticle production and decays assume a five-flavor mass degeneracy of squarks, along with a degeneracy of \tilde{q}_L and \tilde{q}_R states, to avoid potential problems with flavor-changing neutral currents or anomalous parity violation in nuclei. The sparticle couplings are determined by standard model couplings. The only unknowns are the two mass parameters $m(\tilde{q})$ and $m(\tilde{g})$.

Three scenarios have been proposed²⁴⁻²⁷ to account for the \not{p}_T events: (A) squark-pair (with $m_{\tilde{g}} > m_{\tilde{q}}$); (B) gluino-pair (with $m_{\tilde{q}} > m_{\tilde{g}}$); (C) extra-heavy squark (light \tilde{g}). Typical subprocesses for these scenarios are illustrated in Fig. 7. To explain the hardness of the \not{p}_T spectrum a \sqrt{s} threshold of ~ 100 GeV is necessary, which requires sparticle masses of (A) $m_{\tilde{q}} \sim 50$ GeV; (B) $m_{\tilde{g}} \sim 50$ GeV; (C) $m_{\tilde{q}} \sim 100$ GeV with $m_{\tilde{g}} \sim 5$ GeV. In (C) a long \tilde{g} lifetime or a soft $\tilde{g} \rightarrow \tilde{g}$ -hadron fragmentation is needed.

The jets are defined using an algorithm for partons which parallels the UA1 jet algorithm.²³ Partons in descending order of E_T are coalesced into a jet so long as $(\Delta\phi)^2 + (\Delta\eta)^2 < 1$ between the jet axis and the next parton. The fast jet is required to have $p_T > 25$ GeV and other jets $p_T > 12$ GeV. The monojet cross sections obtained in all three scenarios are able to accommodate the observed rate.

More than 50% of the monojets in scenario (A) and nearly all the monojets in (C) are single quarks. These scenarios are therefore better able to account for the low mass and low charged particle multiplicities of the observed monojets than scenario (B), in which the monojets are mainly multi-quarks.

The p_T spectrum of monojet events is broad in scenario (A), sharply decreasing above the p_T cut in scenario (B), and has a Jacobian peak at $m_{\tilde{q}}$ in scenario (C). Again scenarios (A) and (C) seem most consistent with the monojet data; their p_T distributions are shown in Fig. 8.

The predicted dijet cross sections for events with $p_T > 40$ GeV are quite different. In scenario (A) a ratio $\sigma(2j)/\sigma(1j) \sim 2$ is obtained, whereas (C) gives $\sigma(2j)/\sigma(1j) \sim 1/3$; in the latter case the soft- p_T gluino materializes only rarely as an observable jet.

The question has been raised²⁸ as to whether the top quark signal could be faked by the production of squark pairs in scenario (A), decaying via

$$\begin{array}{ccc} \tilde{q} & & \tilde{\bar{q}} \\ \swarrow & & \searrow \\ \tilde{\gamma}q & & \tilde{\omega}\bar{q} \\ & & \searrow \\ & & e\tilde{\nu}, \tilde{e}\nu \end{array}$$

which could give $e + 2$ -jet events. The optimum $\tilde{\omega}$ mass for such top-faking²⁹ is between the \tilde{q} and $\tilde{\nu}$ masses, to obtain a sufficiently large $e + 2$ -jet cross section [e.g. $\tilde{q}(50)$; $\tilde{\omega}(35)$; $\tilde{\nu}(25)$]. However, this mechanism gives large p_T (due to the $\tilde{q} \rightarrow \tilde{\gamma}q$ decay) unlike the observed $e + 2$ -jet events and does not fake most peaks of $W \rightarrow t\bar{b}$ transverse mass distributions. This top-faking mechanism is thus rejected. Of course there is the possibility that sparticle contributions are present in addition to $W \rightarrow t\bar{b}$, in which case we would have the interesting situation of top as the background to other new physics.

Another effect of light sparticles is to increase the W and Z widths by up to 50% of their standard model values.³⁰ The change in Γ_Z/Γ_W in turn

changes the W/Z production ratio

$$R \equiv \frac{[\sigma(W^+) + \sigma(W^-)]B(W \rightarrow e\nu)}{\sigma(Z^0) B(Z \rightarrow e\bar{e})} = \frac{\sigma(W^+) + \sigma(W^-)}{\sigma(Z^0)} \frac{\Gamma_Z \Gamma(W \rightarrow e\nu)}{\Gamma_W \Gamma(Z \rightarrow e\bar{e})}$$

The standard model value is $R = 8.9 \pm 0.5$. With squark masses of 40 GeV and slepton masses of 25 GeV, motivated by scenario (A) and grand unification, the predicted ratio³¹ is $R = 10.5$. The preliminary UA1 upper bound³² (90% C.L.) is $R < 8.7$. Thus R measurements may soon exclude sleptons as light as 25 GeV.

In conclusion, if the UA1 monojets are of supersymmetry origin, then squark and gluino masses are already tightly constrained and dijet events with large p_T should help distinguish between the two most promising scenarios. The top signal is not being faked by sparticles.

5. Acknowledgments

I wish to thank Roger Phillips for comments. I thank H. Baer, W.-Y. Keung, A. D. Martin, R.J.N. Phillips and J. Woodside for collaborations which led to many of the results presented here.

This research was supported in part by the Department of Energy under contract DE-AC02-76ER00881.

6. References

1. F. Halzen, in Proc. XXI Int. Conf. on High Energy Physics, Paris, J. Phys. C3-381 (1982); R.J.N. Phillips, in Proc. of XX Int. Conf. on High Energy Physics, AIP Conf. Proc. 68, 1470 (1981); R. Odorico, Phys. Lett. 118B, 425 (1982); Nucl. Phys. B 209, 77 (1982).
2. V. Barger, H. Baer, K. Hagiwara, A. D. Martin and R.J.N. Phillips, Phys. Rev. D 29, 1923 (1984).
3. I. Schmitt, L. M. Sehgal, H. Tholl and P. Zerwas, Phys. Lett. 139B, 99 (1984); Z. Kunszt, E. Pietarinen and E. Reya, Phys. Rev. D 21, 733 (1980); F. Halzen and P. Hoyer, UW-Madison report PH/224 (1984).
4. C. Peterson, D. Schlatter, I. Schmitt and P. Zerwas, Phys. Rev. D 27, 105 (1983).
5. J. Green et al., Phys. Rev. Lett. 51, 347 (1983); S. E. Csorna et al., Cornell preprint CLNS 85/640.
6. UA1 collaboration: G. Arnison et al., Phys. Lett. 147B, 493 (1984).

7. A. Kernan, private communication at Aspen Winter Conference (1985).
 8. UA1 collaboration: G. Arnison et al., CERN report EP/85-19; N. Ellis, report at Aosta meeting (1985); H.-G. Moser, report at this meeting.
 9. V. Barger and R.J.N. Phillips, UW-Madison report PH/219 (1985); Phys. Lett. 143B, 254 (1984).
 10. A. Ali, report at this meeting; A. Ali and C. Jarlskog, Phys. Lett. 144B, 266 (1984).
 11. V. Barger and R.J.N. Phillips, Phys. Rev. D 31, 215 (1984).
 12. K. Hagiwara and S. Jacobs, UW-Madison report PH/192 (1984); F. Halzen and F. Herzog, Phys. Lett. 151B, 295 (1985); Phys. Rev. D 30, 2326 (1984).
 13. UA1 collaboration: G. Arnison et al., Phys. Lett. 147B, 222 (1984); C. Rubbia, comment from the floor at this meeting.
 14. UA1 collaboration: G. Arnison et al., Phys. Lett. 122B, 103 (1983); 126B, 398 (1983); 134B, 469 (1984). UA2 collaboration: M. Banner et al., Phys. Lett. 122B, 476 (1983); P. Bagnaia et al., Phys. Lett. 129B, 130 (1983).
 15. V. Barger and S. Pakvasa, Phys. Lett. 82B, 445 (1979); G. Kane and M. Peskin, Nucl. Phys. B 195, 29 (1982).
 16. P. Avery et al., Phys. Rev. Lett. 53, 1309 (1984).
 17. V. Barger, A. D. Martin, R.J.N. Phillips, Phys. Lett. 125B, 339, 343 (1984); Phys. Rev. D 28, 145 (1983); V. Barger, H. Baer, A. D. Martin and R.J.N. Phillips, Phys. Rev. D 29, 887 (1984).
 18. M. Abud, R. Gatto and C. A. Savoy, Phys. Lett. 79B, 435 (1978); S. Pakvasa, M. Dechantsreiter, F. Halzen and D. M. Scott, Phys. Rev. D 20, 2862 (1979); R. Horgan and M. Jacob, Phys. Lett. 107B, 395 (1980); N. Cabibbo and L. Maiani, Phys. Lett. 87B, 366 (1979); L. L. Chau, W.-Y. Keung and S.C.C. Ting, Phys. Rev. D 24, 2862 (1980).
 19. R. M. Godbole, S. Pakvasa and D. P. Roy, Phys. Rev. Lett. 50, 1539 (1983); K. Hagiwara and W. F. Long, Phys. Lett. 132B, 202 (1983); L. M. Sehgal and P. Zerwas, Nucl. Phys. B 234, 61 (1984); R. Horgan and M. Jacob, Nucl. Phys. B 238, 221 (1984); D. P. Roy, Zeit. Phys. C 21, 333 (1984); R. M. Godbole and D. P. Roy, Dortmund preprint DO-TH 84/25; B. R. Desai and J. Lindfors, Phys. Lett. 131B, 217 (1983).
 20. N. Minard, report at this meeting.
 21. V. Barger, A. D. Martin and R.J.N. Phillips, Phys. Lett. 151B, 463 (1985).
-

22. V. Barger, H. Baer, K. Hagiwara and R.J.N. Phillips, Phys. Rev. D 30, 947 (1984).
23. UA1 collaboration: G. Arnison et al., Phys. Lett. 139B, 115 (1984); M. Mohammadi, report at Aspen Winter Conference (1985).
24. V. Barger, K. Hagiwara and W.-Y. Keung, Phys. Lett. 145B, 147 (1984); J. Ellis and H. Kowalski, Nucl. Phys. B 246, 189 (1984); A. R. Allan, E.W.N. Glover and A. D. Martin, Phys. Lett. 146B, 247 (1984); H. E. Haber and G. L. Kane, Phys. Lett. 142B, 212 (1984); V. Barger, K. Hagiwara, W.-Y. Keung, R.J.N. Phillips and J. Woodside, UW-Madison report PH/230 (1985).
25. E. Reya and D. P. Roy, Phys. Lett. 141B, 442 (1984); Phys. Rev. Lett. 52, 881 (1984); J. Ellis and H. Kowalski, Phys. Lett. 142B, 441 (1984).
26. V. Barger, K. Hagiwara, W.-Y. Keung and J. Woodside, Phys. Rev. Lett. 53, 641 (1984); M. J. Herrero, K. Ibáñez, C. López and F. Yndurain, Phys. Lett. 132B, 199 (1983); 145B, 430 (1984); R. M. Barnett, H. E. Haber and G. L. Kane, LBL report 18990 (1985); A. DeRújula and R. Petronzio, CERN report TH.4070/84; V. Barger, K. Hagiwara, S. Jacobs and J. Woodside, UW-Madison report PH/232 (1985).
27. V. Barger, K. Hagiwara, W.-Y. Keung and J. Woodside, Phys. Rev. D 31, 528 (1985); M. Glück, E. Reya and D. P. Roy, Dortmund preprint 85/1 (1985); J. Ellis and H. Kowalski, CERN report TH.4072 (1984).
28. L. Hall and S. Raby, Harvard preprint HUTP-84/A074.
29. V. Barger, W.-Y. Keung and R.J.N. Phillips, UW-Madison report PH/228 (1985); see also H. Baer and X. Tata, CERN report TH.4147 (1985); M. Glück and E. Reya, Phys. Rev. Lett. 51, 867 (1983).
30. V. Barger, R. W. Robinett, W.-Y. Keung and R.J.N. Phillips, Phys. Rev. D 28, 2192 (1983).
31. N. Deshpande, G. Eilam, V. Barger and F. Halzen, Phys. Rev. Lett. 54, 1757 (1985).
32. V. Vuillemin, report at Aspen Winter Conference (1985).

7. Figure Captions

- Fig. 1. Comparison of inclusive muon p_T distribution from heavy-quark fusion and electroweak subprocesses with UA1 measurements from Ref. 6.
- Fig. 2. Two-dimensional zone plots from Ref. 9 of dimuon cross sections (in pb) at $\sqrt{s} = 630$ GeV from combined c and b quark contributions (a) unlike-sign dimuons, (b) like-sign dimuons (no mixing).

- Fig. 3. Inclusive jet cross sections at $\sqrt{s} = 540$ GeV with $|\eta| \leq 1$ calculated in Ref. 11 from low-order QCD and electroweak subprocesses.
- Fig. 4. Perturbative QCD calculation of charm in jets from Ref. 11 compared to the early UA1 data from Ref. 13.
- Fig. 5. Transverse mass distributions for $W \rightarrow t\bar{b}$ events with $t \rightarrow b\nu$ decay (see Refs. 17, 21).
- Fig. 6. Comparison of $W \rightarrow t\bar{b}$ and $t\bar{t}$ predictions from Ref. 21 for transverse and invariant mass distributions in $e(\mu) + 2$ -jet events with the 1983 UA1 t-candidate events of Ref. 6.
- Fig. 7. Typical subprocesses in the three supersymmetry scenarios proposed to explain the UA1 monojets.
- Fig. 8. Predicted p_T distributions of monojets in the squark pair and extra-heavy squark scenarios; the arrows (asterisks) along the top denote p_T values of the UA1 monojet events from the 1984 (1983) runs. The calculations do not include p_T resolution smearing.
-

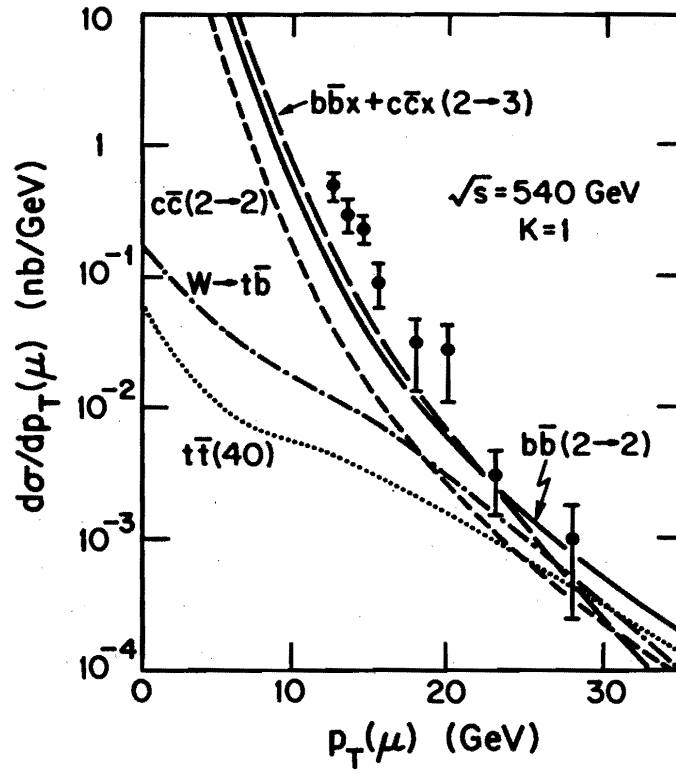


Fig. 1

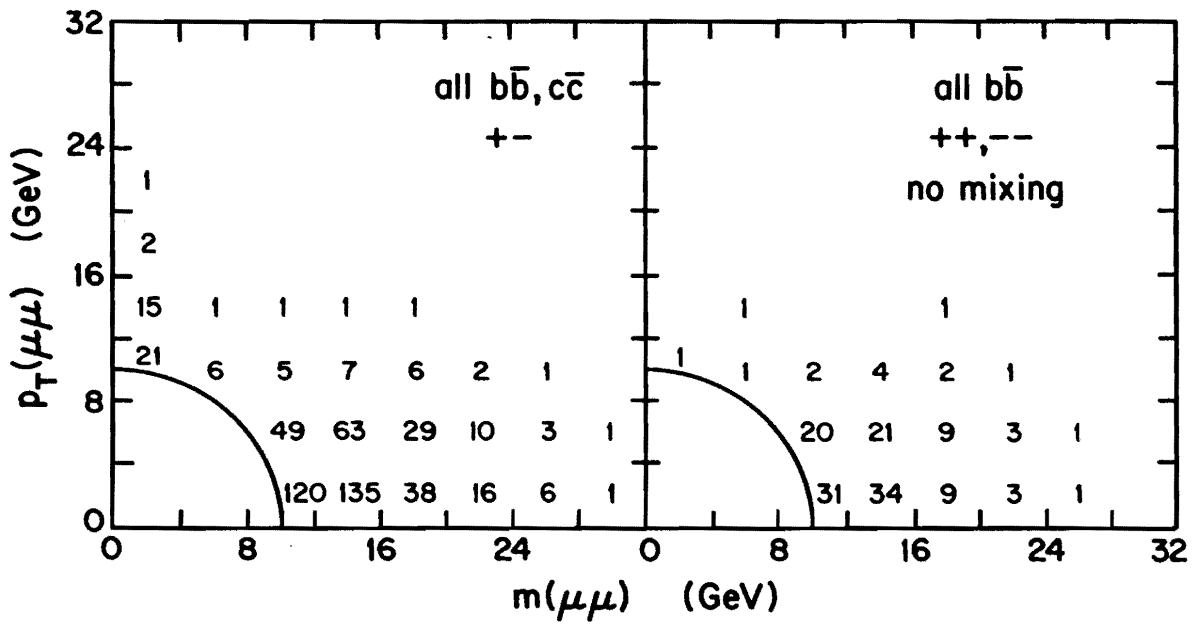


Fig. 2

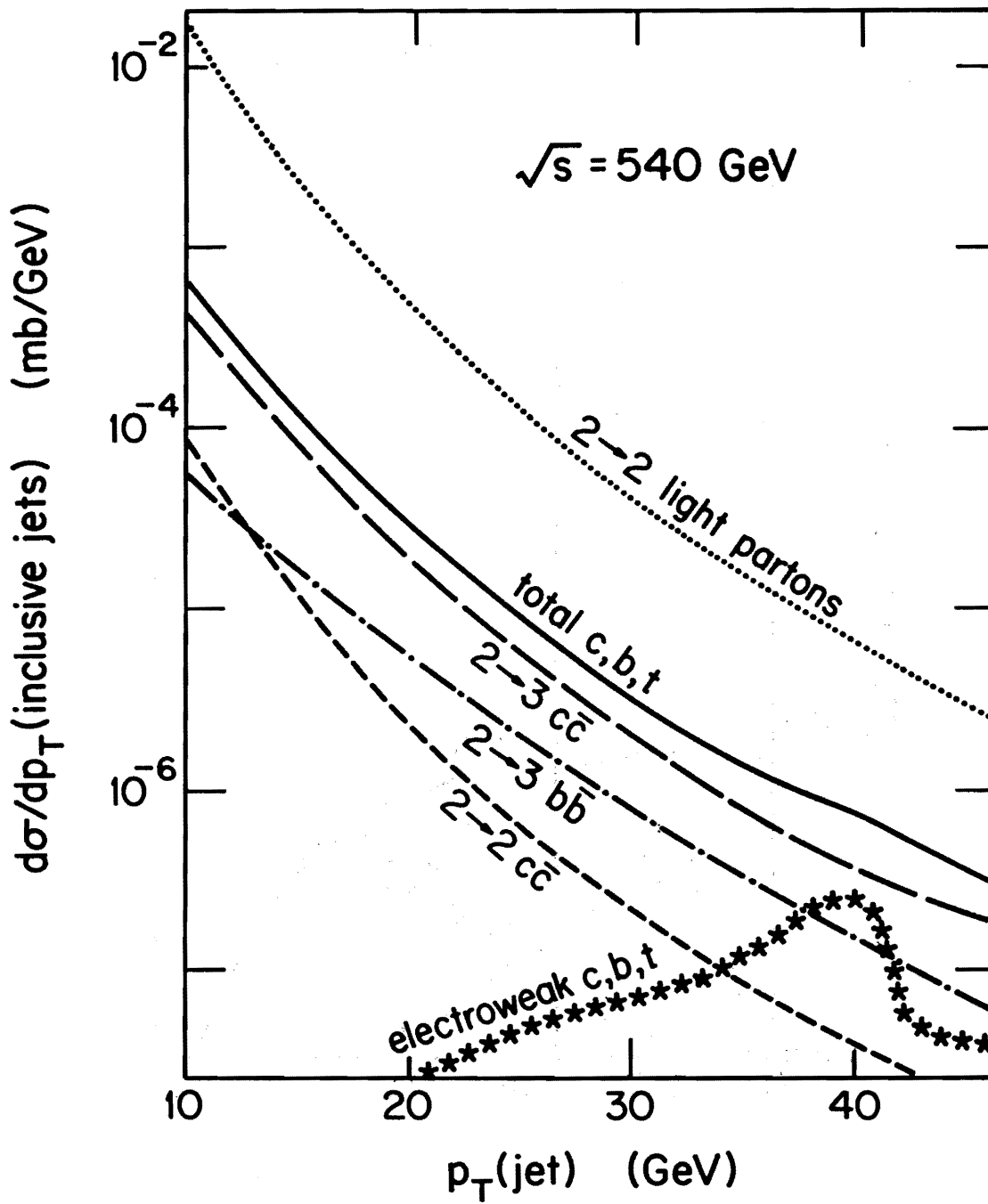


Fig. 3

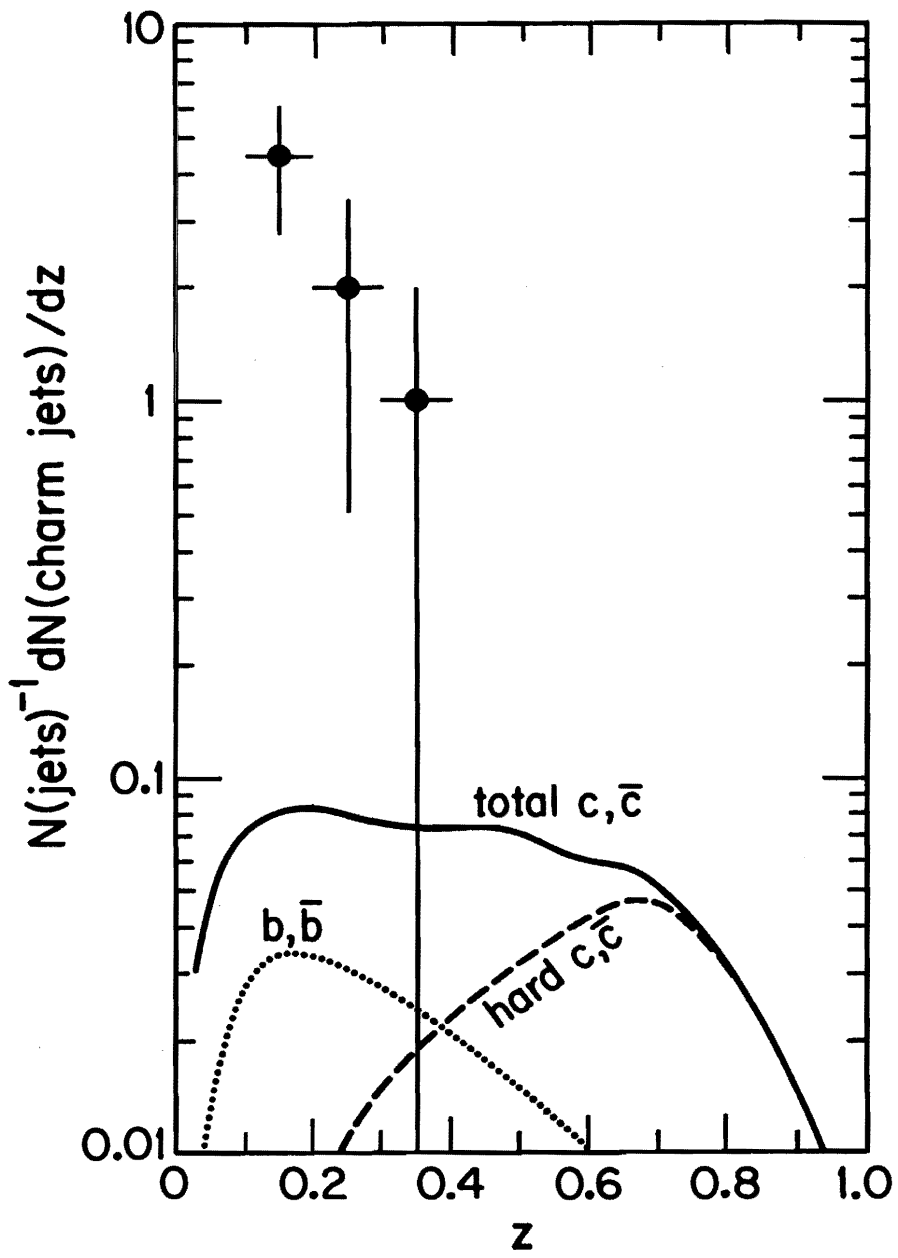


Fig. 4

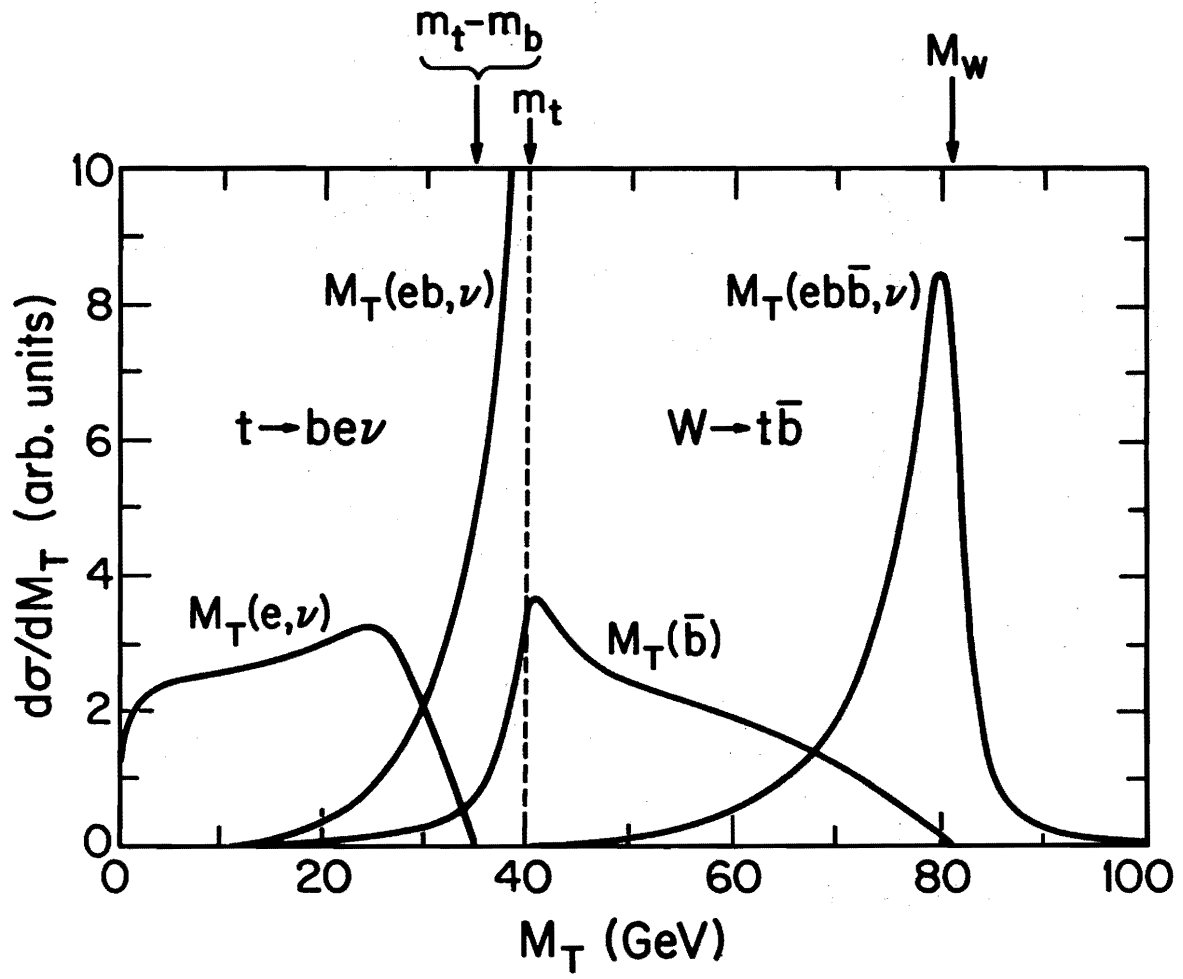


Fig. 5

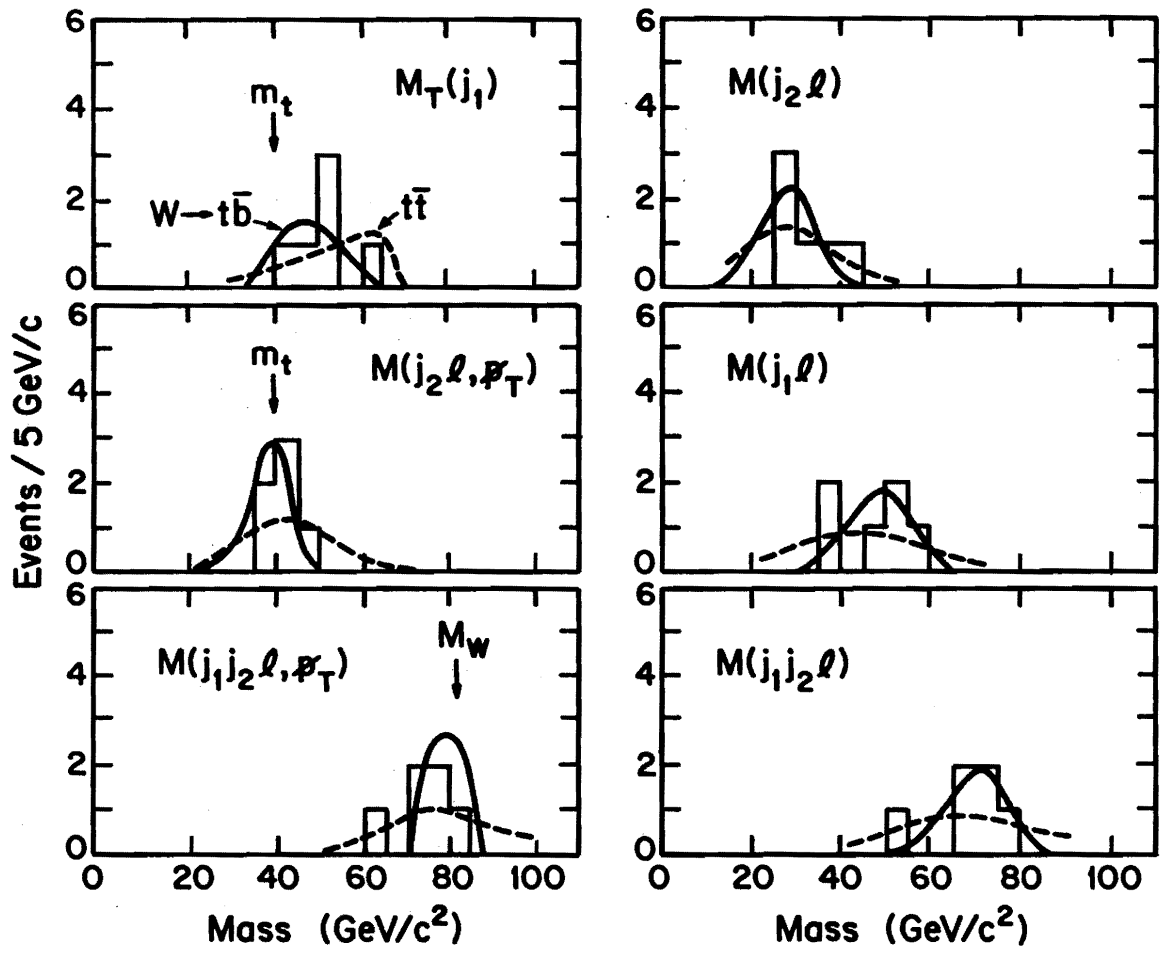


Fig.6

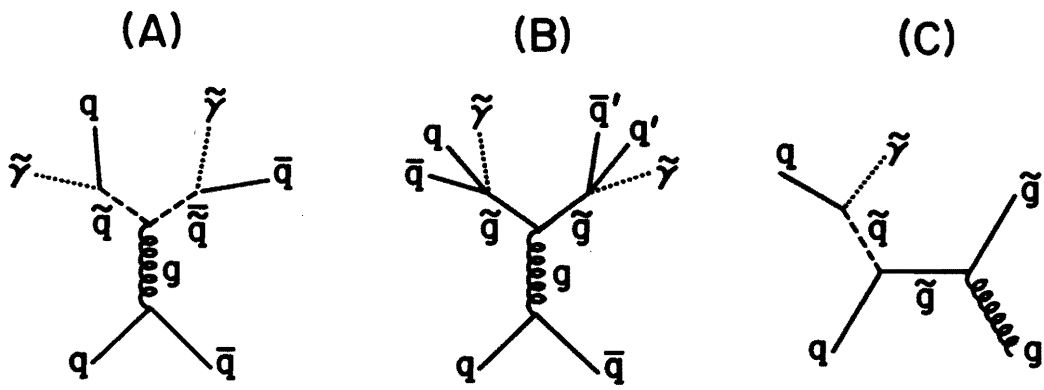


Fig. 7

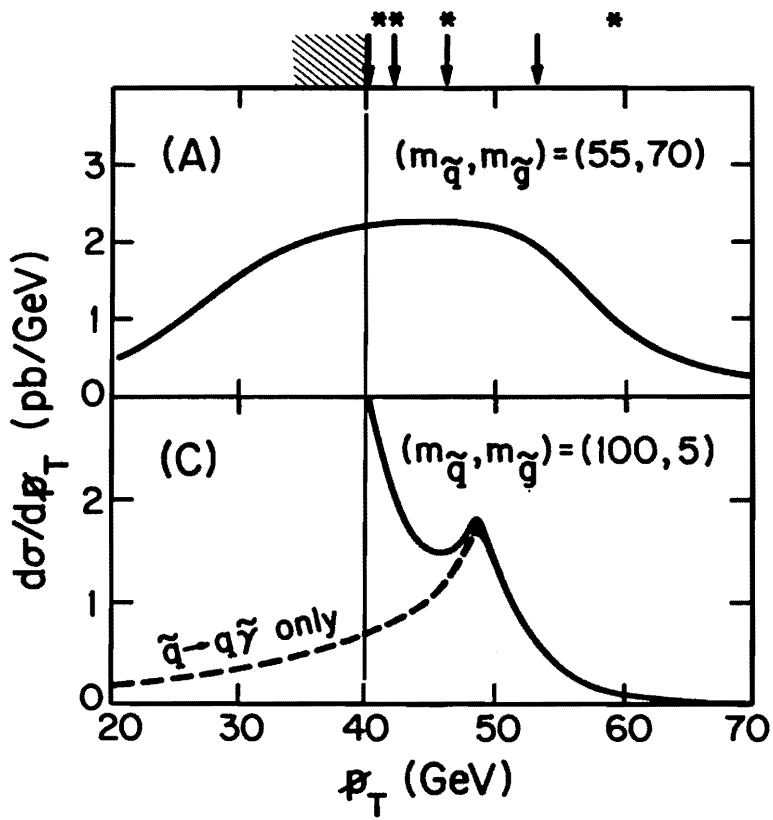


Fig. 8